

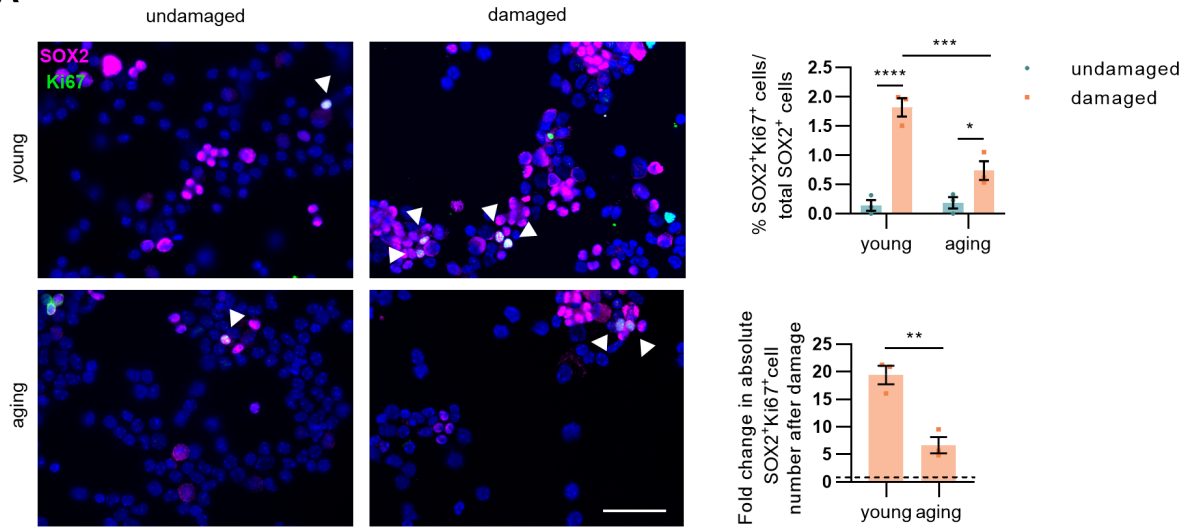
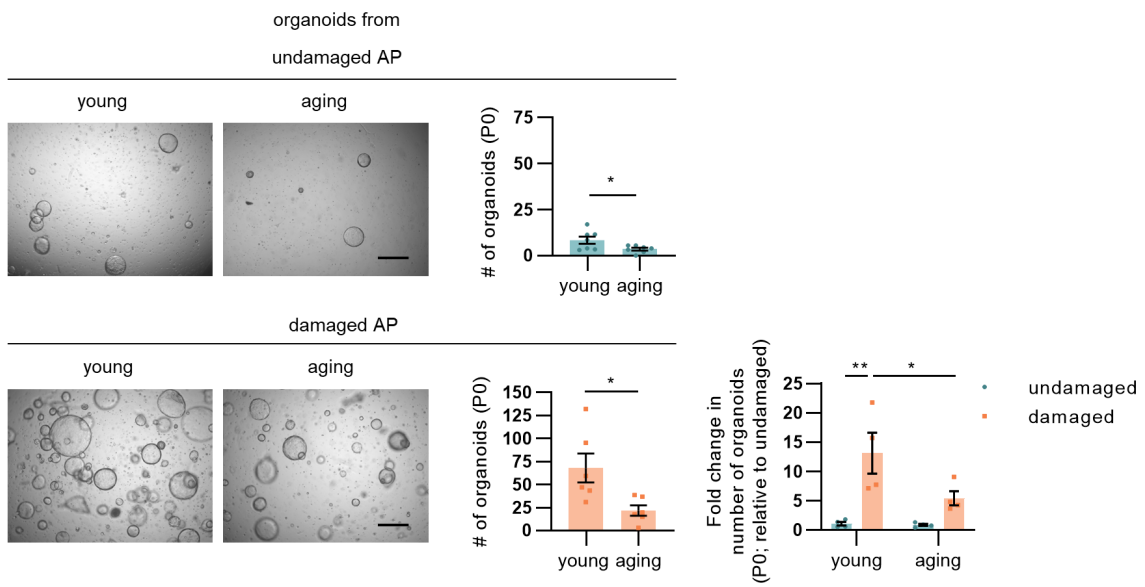
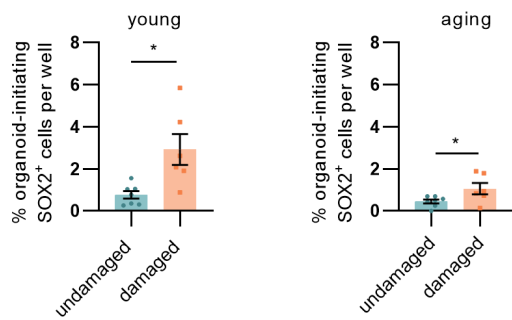
Interleukin-6 is an activator of pituitary stem cells upon local damage, a competence quenched in the aging gland

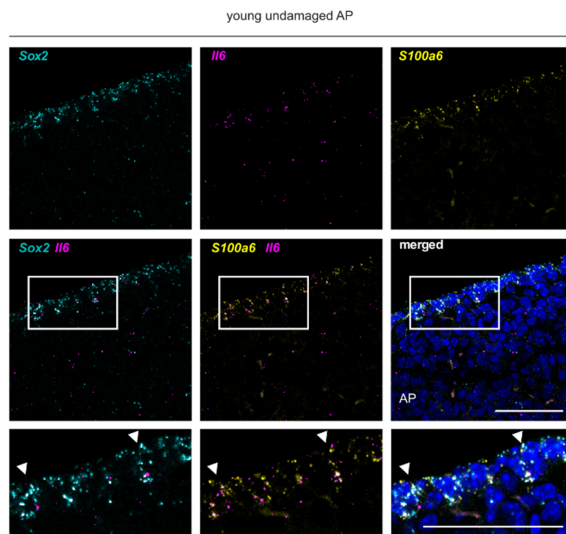
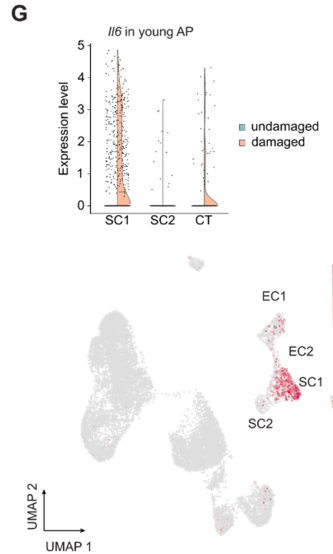
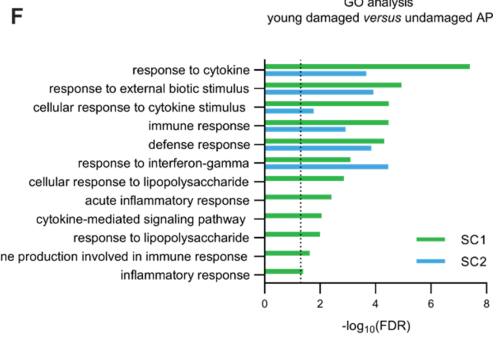
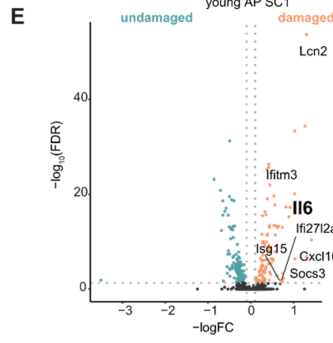
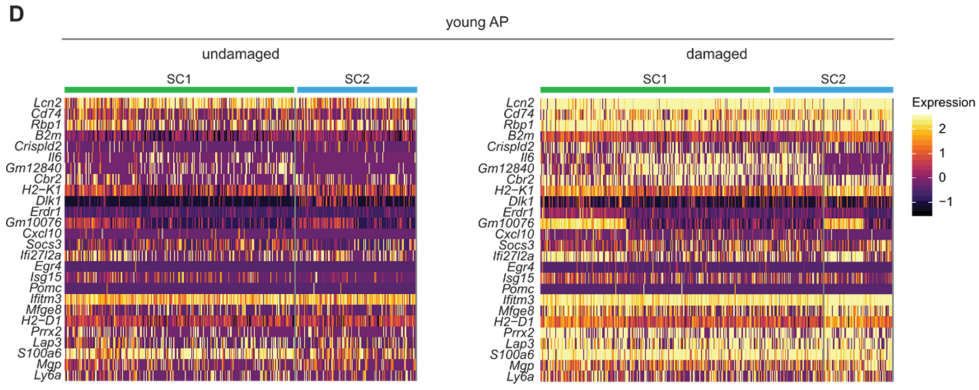
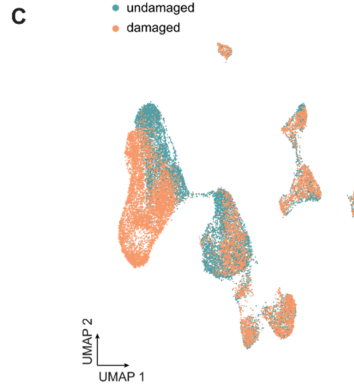
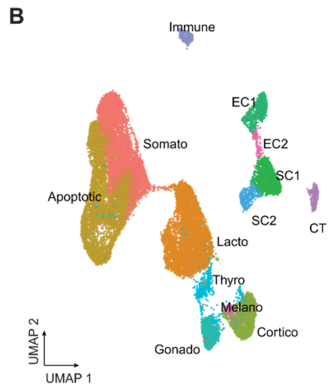
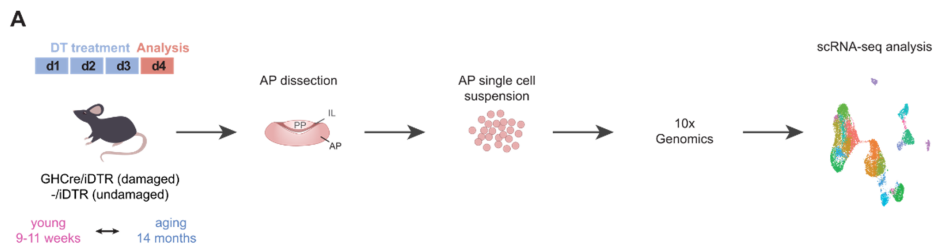
Peer-reviewed author version

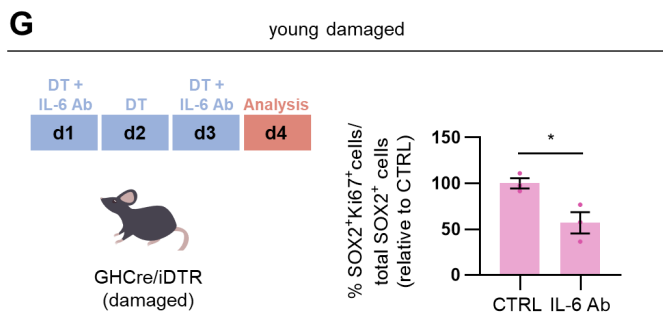
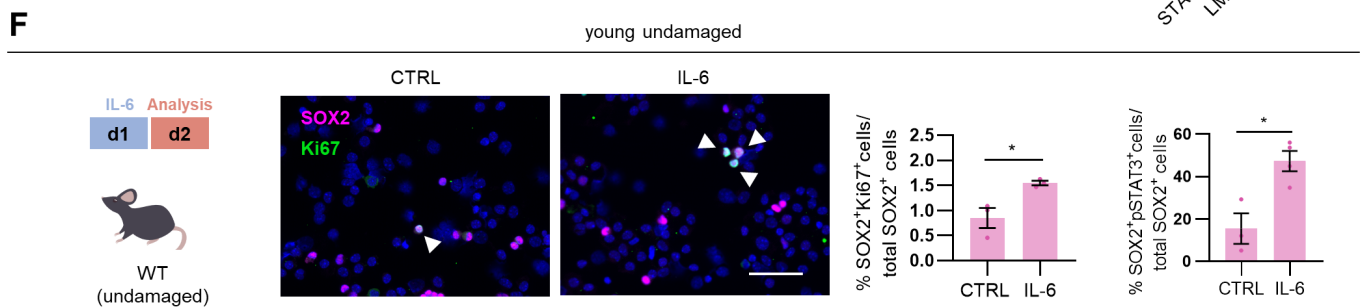
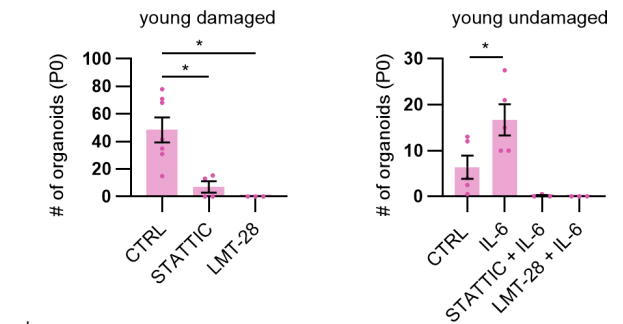
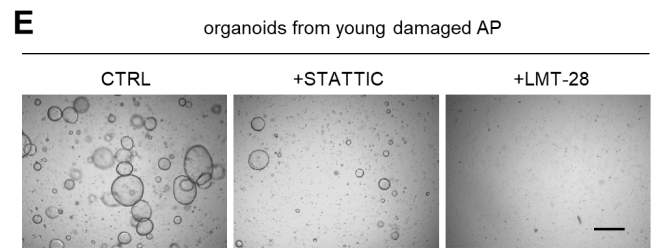
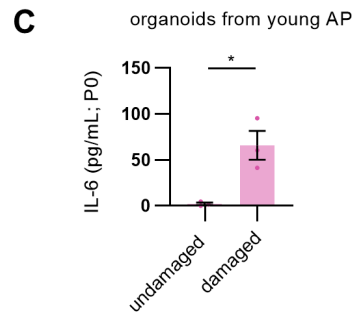
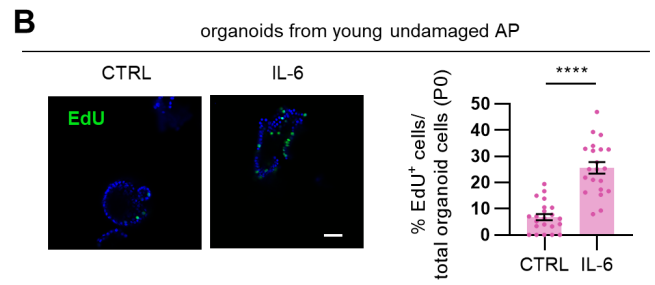
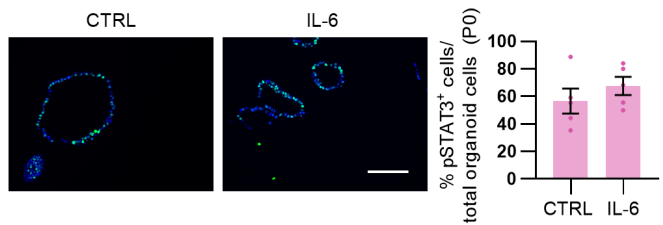
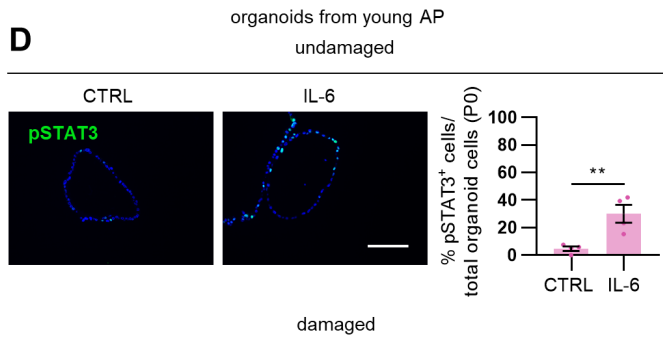
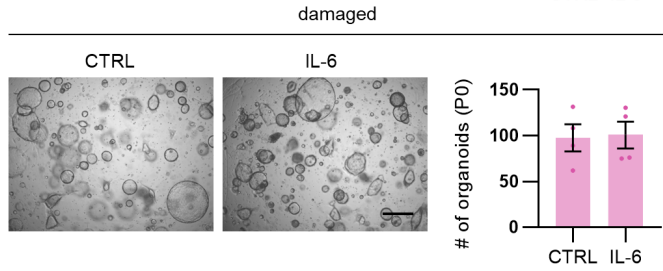
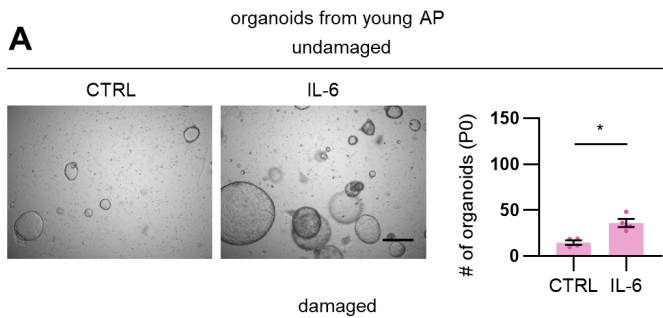
Vennekens, A; Laporte , E; HERMANS, Florian; Cox , B; Modave, E; Janiszewski, A; Nys, C; Kobayashi, H; Malengier-Devlies, B; Chappell, J; Matthys , P; Garcia, MI; Pasque, V; Lambrechts, D & Vankelecom, H (2021) Interleukin-6 is an activator of pituitary stem cells upon local damage, a competence quenched in the aging gland. In: Proceedings of the National Academy of Sciences of the United States of America, 118 (25) (Art N° e2100052118).

DOI: 10.1073/pnas.2100052118

Handle: <http://hdl.handle.net/1942/35883>

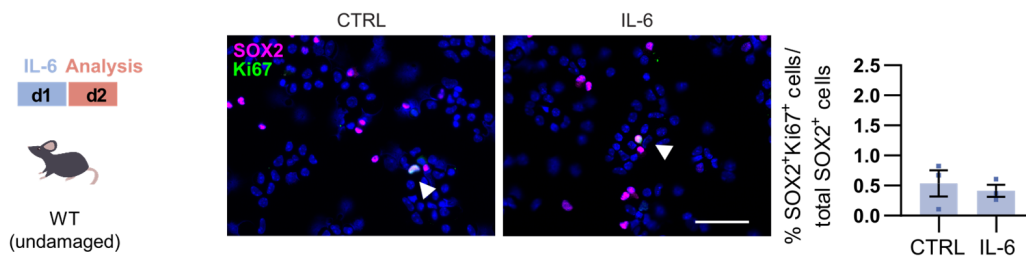
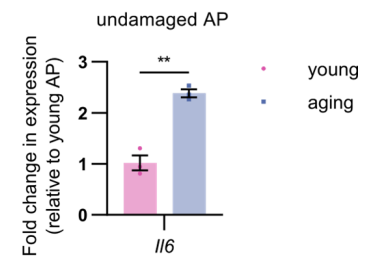
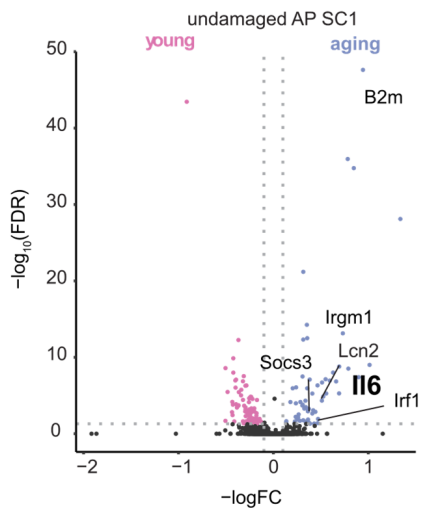
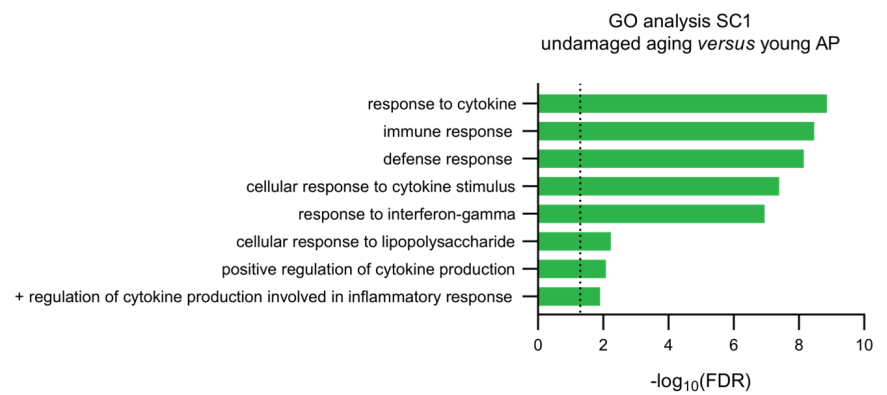
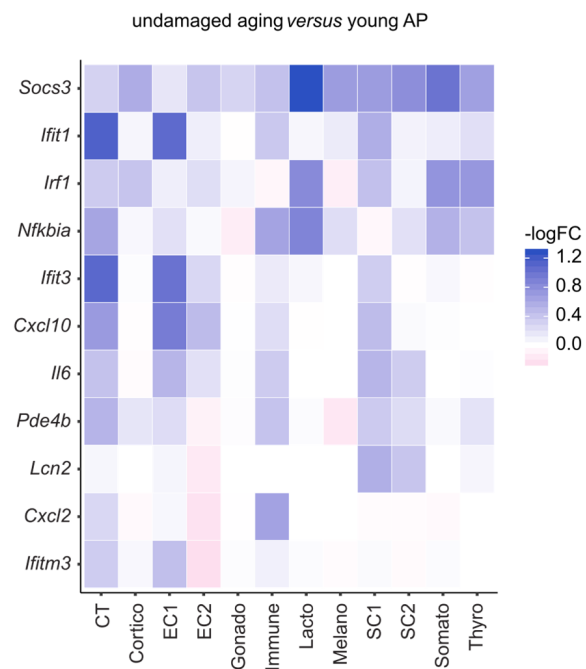
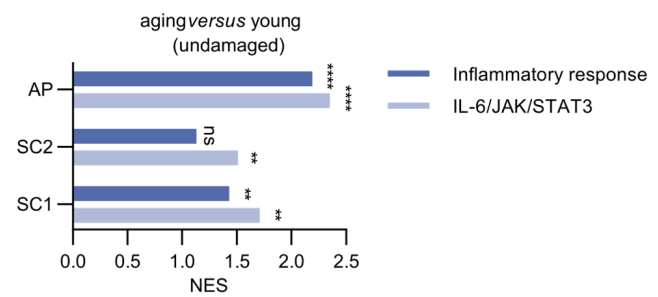
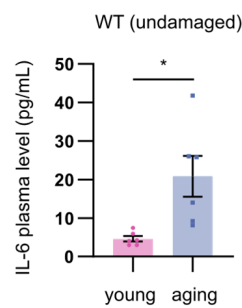
A**B****C**

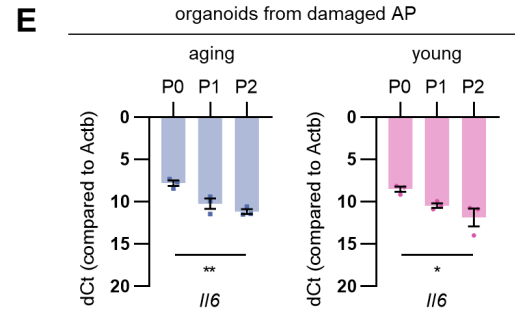
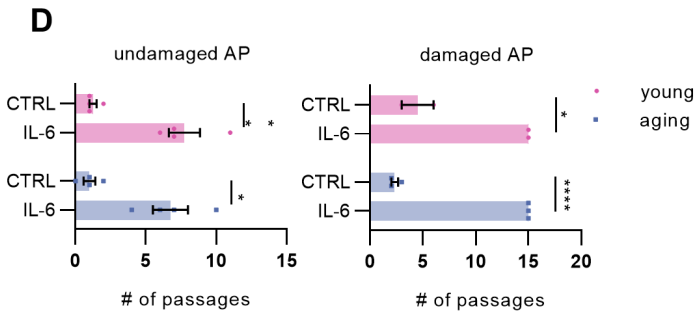
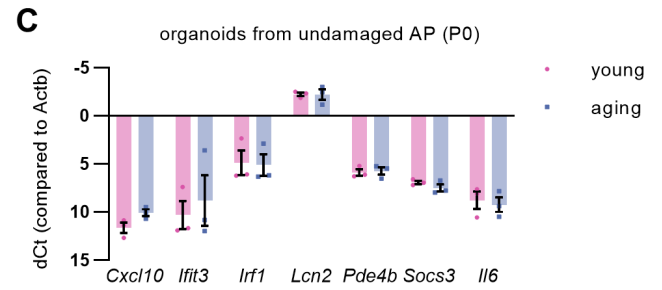
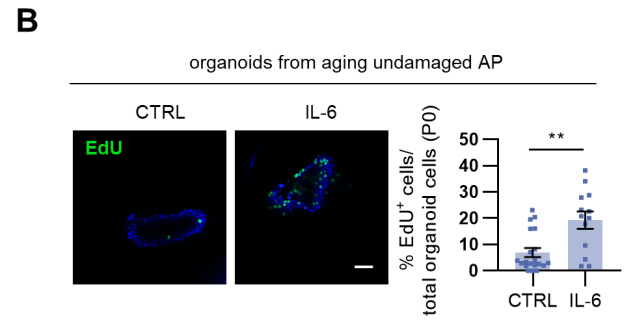
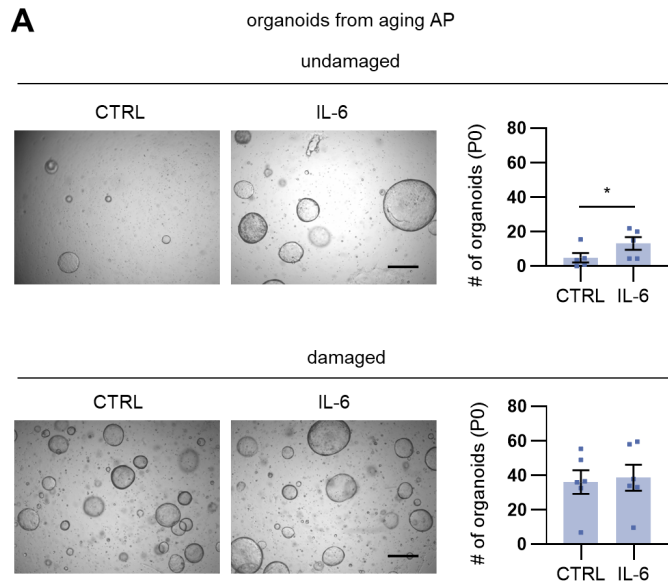




A

aging undamaged

**B****C****D****E****F****G**



Main Manuscript for

Interleukin-6 is an activator of pituitary stem cells upon local damage, a competence quenched in the aging gland

- 1 Annelies Vennekens^{1*}, Emma Laporte^{1*}, Florian Hermans^{1,2}, Benoit Cox¹, Elodie Modave^{3,4},
2 Adrian Janiszewski⁵, Charlotte Nys¹, Hiroto Kobayashi^{1,6}, Bert Malengier-Devlies⁷, Joel
3 Chappell⁵, Patrick Matthys⁷, Marie-Isabelle Garcia⁸, Vincent Pasque⁵, Diether Lambrechts^{3,9},
4 Hugo Vankelecom^{1,#}

¹Laboratory of Tissue Plasticity in Health and Disease, Cluster of Stem Cell and Developmental Biology, Department of Development and Regeneration, Leuven Stem Cell Institute, KU Leuven (University of Leuven), Leuven, Belgium

²Laboratory of Morphology, Biomedical Research Institute, Hasselt University, Diepenbeek, Belgium

³Center for Cancer Biology, VIB, Leuven, Belgium

⁴Laboratory for Intestinal Neuroimmune Interactions, Translational Research Center for Gastrointestinal Disorders, Department of Chronic Diseases, Metabolism and Ageing, KU Leuven, Leuven, Belgium

⁵Laboratory for Cellular Reprogramming and Epigenetic Regulation, Cluster of Stem Cell and Developmental Biology, Department of Development and Regeneration, Leuven Stem Cell Institute, KU Leuven, Leuven, Belgium

⁶Department of Anatomy and Structural Science, Yamagata University Faculty of Medicine, Yamagata, Japan

⁷Immunity and Inflammation Research Group, Department of Microbiology, Immunology and Transplantation, KU Leuven, Leuven, Belgium

⁸Institut de Recherche Interdisciplinaire en Biologie Humaine et Moléculaire (IRIBHM), Faculty of Medicine, Université Libre de Bruxelles (ULB), Brussels, Belgium

⁹Laboratory for Translational Genetics, Department of Human Genetics, KU Leuven, Leuven, Belgium

*Both authors contributed equally

#Corresponding author: Hugo Vankelecom

Email: hugo.vankelecom@kuleuven.be

Hugo Vankelecom: 0000-0002-2251-7284

Annelies Vennekens: 0000-0001-6278-251X

Emma Laporte: 0000-0003-0799-3116

Florian Hermans: 0000-0002-2321-3995

Benoit Cox: 0000-0002-3139-268X

Elodie Modave: 0000-0002-5775-3332
Adrian Janiszewski: 0000-0002-4156-5791
Charlotte Nys: 0000-0001-8917-7934
Bert Malengier-Devlies: 0000-0003-3527-1145
Joel Chappell: 0000-0002-5834-4100
Patrick Matthys: 0000-0002-9685-6836
Marie-Isabelle Garcia: 0000-0003-2147-7003
Vincent Pasque: 0000-0002-5129-0146
Diether Lambrechts: 0000-0002-3429-302X

Classification

Major category: Biological Sciences
Minor category: Cell Biology

Keywords

pituitary; stem cells; interleukin-6; aging; organoids

Author Contributions

A.V. and E.L. designed the concepts and experiments, performed the experiments, analyzed the data, interpreted the results and co-wrote the manuscript; F.H. processed scRNA-seq data and regulon analysis, and assisted in confocal imaging of organoids; B.C. provided pituitary organoid expertise and data, and assisted in experimental set-up; E.M. performed initial scRNA-seq bioinformatic processing; A.J. assisted in scRNA-seq analysis and co-performed regulon analysis; C.N. helped with specific organoid experiments; H.K. performed and co-interpreted transmission electron microscopy; B.M-D. assisted in immune cell- and cytokine-related analyses; J.C. assisted in scRNA-seq analysis; P.M. supervised immune cell- and cytokine-related analyses; M-I.G. contributed to specific immunostaining experiments; V.P. co-supervised scRNA-seq and regulon analysis; D.L. co-supervised scRNA-seq experiments and analysis; H.V. supervised the entire project, co-developed the concepts and ideas, co-designed the experiments, co-interpreted the data and wrote the manuscript. All authors critically reviewed and approved the manuscript.

This PDF file includes:

Main Text
Legends to Figures

5 **Abstract**

6 Stem cells in the adult pituitary are quiescent, yet show acute activation upon tissue injury.
7 Molecular mechanisms underlying this reaction are completely unknown. We applied single-cell
8 transcriptomics to start unraveling the acute pituitary stem cell activation process as occurring
9 upon targeted endocrine cell-ablation damage. This stem cell reaction was contrasted to aging
10 (middle-aged) pituitary, known to have lost damage-repair capacity.

11 Stem cells in aging pituitary show regressed proliferative activation upon injury and diminished *in*
12 *vitro* organoid formation. Single-cell RNA sequencing (scRNA-seq) uncovered interleukin-6 (IL-6)
13 as being upregulated upon damage, however only in young but not aging pituitary. Administering
14 IL-6 to young mice promptly triggered pituitary stem cell proliferation, while blocking IL-6 or
15 associated signaling pathways inhibited such reaction to damage. By contrast, IL-6 did not
16 generate a pituitary stem cell activation response in aging mice, coinciding with elevated basal IL-
17 6 levels and raised inflammatory nature in the aging gland (inflammaging). Intriguingly, *in vitro*
18 stem cell activation by IL-6 was not only discerned in organoid culture from young but also aging
19 pituitary, indicating that the aging gland's stem cells retain intrinsic activatability, *in vivo* likely
20 impeded by the prevailing inflammatory tissue milieu. Importantly, IL-6 supplementation strongly
21 enhanced the growth capability of pituitary stem cell organoids, thereby expanding their potential
22 as experimental model.

23 Together, our study identifies IL-6 as pituitary stem cell activator upon local damage, a
24 competence quenched at aging concomitant with raised IL-6/inflammatory level in the older
25 gland. These new insights may open the way to interfering with pituitary aging.

26 **Significance**

27 The pituitary is the body's master endocrine gland. Local damage and aging present important
28 threats. We started to decrypt the yet ill-defined regulation of the gland's stem cells, typically
29 dormant but acutely activated upon damage. Single-cell transcriptomics uncovered interleukin-6
30 as pituitary stem cell activator upon local damage, corroborated *in vivo* and *in vitro* using stem
31 cell-derived organoids. This competence extinguishes at aging, concurrent with raised

32 inflammatory state in the older gland (inflammaging). However, the aging pituitary's stem cells
33 retain intrinsic activatability, re-surfacing once released from their impeding tissue milieu. Our
34 new insights may instigate tactics to refrain the pituitary from aging, or rejuvenate the aging
35 gland. The single-cell transcriptomic database provides a powerful resource to decipher pituitary
36 damage and aging.

37 **Introduction**

38 The pituitary gland is the key orchestrator of the endocrine system, translating central and
39 peripheral inputs into strictly regulated hormone outputs. Consequently, this master gland steers
40 a multitude of fundamental processes including body growth, metabolism, sexual development,
41 reproduction and stress management. To exert this crucial function, the pituitary encompasses
42 specialized hormone-producing cell types, mainly located in the anterior lobe of the gland
43 (anterior pituitary, AP) and comprising somatotropes (producing growth hormone (GH)),
44 lactotropes (prolactin (PRL)), corticotropes (adrenocorticotrophic hormone (ACTH)), gonadotropes
45 (luteinizing hormone (LH) and/or follicle-stimulating hormone (FSH)) and thyrotropes (thyroid-
46 stimulating hormone (TSH)). On top, the pituitary contains a population of stem cells, essentially
47 marked by sex determining region Y-box 2 (SOX2) expression (1–4). The physiological role of the
48 pituitary stem cells remains poorly understood (5, 6). Transgenic SOX2 lineage tracing revealed
49 involvement in adult gland homeostasis and adaptation to altered endocrine demands, although
50 contributions were not large (3, 4). Progressively, the picture emerges that adult pituitary stem
51 cells are mainly dormant and not predominantly involved in tissue homeostasis and physiological
52 remodeling (7–9), reminiscent of findings in other tissues with comparable low-turnover rates
53 (such as muscle and liver; (10, 11)). Yet, in case of damage in the adult pituitary, the resident
54 stem cell compartment shows swift activation (12, 13). More in particular, following diphtheria
55 toxin (DT)-triggered endocrine cell-ablation injury in the G_HCre/iDTR mouse model (expressing
56 the Cre recombinase under control of the *Gh* promoter, as well as the Cre-inducible DT receptor
57 (iDTR)), the pituitary stem cell population is promptly activated displaying enhanced proliferative
58 activity and expansion (12). Substantial regeneration of the obliterated somatotropes is eventually
59 observed after 5 to 6 months (12). Surprisingly, this regenerative competence of the gland rapidly

60 drops with aging, being not observed anymore when mice reach middle age (from 8-10 months of
61 age; (14)).

62 Virtually nothing is known about the molecular machinery driving the quiescent pituitary stem cells
63 into activation (as observed following local injury), neither about how this route may change at
64 advancing age. In other tissues, it was found that stem cells undergo an intrinsic aging process
65 (such as in the hematopoietic system; (15)), or regress in functionality because of the aging
66 tissue milieu (as described in muscle and brain; (16–18)). Here, we started to tackle this query by
67 interrogating young-adult and aging (middle-aged), damaged and undamaged pituitary
68 (specifically, its major endocrine AP lobe) using single-cell transcriptomics. We focused on the
69 prompt stem cell reaction that occurs immediately upon the DT-induced local damage in the
70 *GHCre/iDTR* model, and substantiated transcriptomic findings using *in vivo* and *in vitro*
71 exploration. To achieve the latter, we applied our recently developed mouse AP-derived organoid
72 model (19). These organoids originate from the (SOX2⁺) stem cells and maintain the pituitary
73 stem cell phenotype in culture. Moreover, growth characteristics reflect the stem cells' activation
74 (as observed following damage and at neonatal age), and organoid-based findings were found
75 reliably translatable to the *in vivo* situation (19). Hence, this organoid system provides an
76 interesting *in vitro* pituitary stem cell biology/activation readout tool.

77 In the present study, we identified interleukin-6 (IL-6) to be upregulated in the young pituitary
78 following tissue injury, and uncovered its pituitary stem cell-activating competence, which
79 however is quenched at aging concomitant with a raised inflammatory nature in the older gland.
80 When released from the *in situ* microenvironment through organoid culturing, the aging pituitary's
81 stem cells regain activatability. These new insights may be harnessed to combat pituitary aging
82 and concomitant regenerative decline.

83 **Results**

84 **Acute proliferative activation of the pituitary stem cells upon local injury subsides at aging**

85 To controllably inflict injury in the pituitary, we used our previously designed *GHCre/iDTR*
86 transgenic mouse model (12) (see Extended Methods). *GH^{Cre/+};R26^{iDTR/+}* mice (further referred to
87 as *GHCre/iDTR*) and control *GH^{+/+};R26^{iDTR/+}* animals (further referred to as *-iDTR*) were injected

88 with DT for 3 days, causing local tissue damage in the GHC*re*/iDTR pituitary by inducing
89 apoptosis in endocrine cells (in particular, somatotropes and lactotropes; (12)). In accord with our
90 previous findings (12), the resident SOX2⁺ stem cells of the young-adult pituitary (8-12 weeks old
91 mice, further referred to as 'young') show an acute increase in proliferative activity (as assessed
92 by Ki67 immunostaining; Fig. 1A) and ensuing expansion of SOX2⁺ cell number (*SI Appendix*,
93 Fig. S1A). This prompt pituitary stem cell activation is significantly lower at older age (10-15
94 months old, middle-aged mice, further referred to as 'aging') (Fig. 1A; *SI Appendix*, Fig. S1A). In
95 addition, the aging basal pituitary houses a reduced number of SOX2⁺ stem cells when compared
96 to the young gland (*SI Appendix*, Fig. S1A), consistent with prior findings (14).

97 Recently, we established an *in vitro* organoid model starting from mouse pituitary (particularly,
98 from the AP) which recapitulates biology and activation of the pituitary stem cells (19). The
99 organoids develop from the SOX2⁺ stem cells as shown before for young AP (19), and
100 demonstrated here for aging pituitary using SOX2^{eGFP/+} reporter-mouse AP giving rise to only
101 eGFP⁺ organoids (*SI Appendix*, Fig. S1B). In addition, when starting from a mixture of cells from
102 SOX2^{eGFP/+} and non-fluorescent wildtype (WT) aging AP, the developing organoids are either
103 entirely fluorescent or non-fluorescent (*SI Appendix*, Fig. S1B), thereby supporting a clonal origin.
104 Moreover, the organoids display a pituitary stemness phenotype in culture, both from young AP
105 (see (19)) and from aging gland (*SI Appendix*, Fig. S1C), expressing known pituitary stem cell
106 markers (SOX2, E-cadherin, cytokeratin-8/18; (19)), and showing absence of hormone-secretory
107 granules and presence of microvilli, similar to the pituitary stem cells as present in the cleft-lining
108 marginal zone (MZ) (*SI Appendix*, Fig. S1D). Using this model system as pituitary stem cell
109 biology and activation readout (19), we observed that primary organoid formation efficiency
110 (referred to as passage 0 or P0) from the aging pituitary is lower than from the young gland, and
111 that the increase in organoid development capacity upon damage is less pronounced at the older
112 age (Fig. 1B), both findings in line with the *in vivo* observations of regressed stem cell number
113 and inferior activation response in aging *versus* young pituitary. Because the endocrine cell
114 ablation in the damaged pituitary, together with the expansion of the SOX2⁺ cell population,
115 entails that a higher absolute number of SOX2⁺ stem cells is seeded per well (i.e. per 10,000 AP

116 cells) from damaged than from undamaged gland, we determined the number of organoid-
117 initiating SOX2⁺ stem cells by normalizing for the calculated SOX2⁺ cell numbers seeded (see
118 Extended Methods). Similar conclusions were reached, showing an increase upon injury at both
119 ages (indicative of stem cell activation), but again less prominent at older age (Fig. 1C).

120 **Single-cell transcriptomics uncovers interleukin-6 to be upregulated in young pituitary** 121 **upon damage**

122 To in detail search for molecular underpinnings of the damage-induced pituitary stem cell
123 response, and of the subsided reaction in the aging gland, we applied single-cell transcriptomics
124 to the different pituitary conditions (i.e. young and aging, damaged and undamaged AP; Fig. 2A).
125 After filtering out dead and low-quality cells, potential doublets and 'background' (ambient) RNA
126 (*SI Appendix*, Fig. S2A and Extended Methods), applied collectively on all single-cell RNA
127 sequencing (scRNA-seq) data obtained in this study (i.e. from young and aging, damaged and
128 undamaged AP, in total yielding 26,115 good-quality cells), unsupervised clustering and
129 visualization using Uniform Manifold Approximation and Projection (UMAP; (20)) were performed
130 (*SI Appendix*, Fig. S2B). Subsequent superposition of canonical lineage markers exposed all
131 known pituitary hormone-producing cell populations (Fig. 2B, Dataset S1 and *SI Appendix*, Fig.
132 S2B). In addition, a connective tissue cluster (annotated in analogy to (21), and indicated with
133 CT) and immune cell cluster were distinguished, as well as an endothelial and stem cell
134 population, both subdivided in two subclusters (Fig. 2B). The endothelial cell subcluster 1 (EC1)
135 shows more expression of mature endothelial cell markers than EC2 (Dataset S1 and *SI*
136 *Appendix*, Fig. S2C), and a first basic mining of the stem cell population revealed that the
137 subclusters (referred to as SC1 and SC2) differ in expression levels of several (pituitary)
138 stemness markers (Dataset S1 and *SI Appendix*, Fig. S2D). Finally, a population of dying
139 (apoptotic) cells was identified, being the result of the DT-induced apoptotic process in the
140 GHC*re*/iDTR (damaged) AP, also included in the unsupervised clustering of the aggregate data
141 (Fig. 2A-C). Of note, a small cluster of melanotrope cells (housed in the intermediate lobe (IL) of
142 the pituitary) was also observed (Fig. 2B; *SI Appendix*, Fig. S2B), likely representing some limited
143 IL tissue still attached to the AP after the latter's isolation from the mouse. Our cell-type

144 categorization outcome, as described above, was validated by performing the clustering based on
145 regulon activity (i.e. transcription factors taken together with their positively regulated target
146 genes) instead of based on differential gene expression (as in Fig. 2B), by applying 'single-cell
147 regulatory network inference' (SCENIC; (22)). This alternative approach resulted in an analogous
148 cell-type categorization pattern (*SI Appendix*, Fig. S2E). Moreover, integrating recently published
149 pituitary scRNA-seq data of comparable mouse age, gender and strain (i.e. young wildtype
150 C57/Bl6 male; (21, 23)) with our equivalent dataset showed prominent correlation (*SI Appendix*,
151 Fig. S2F).

152 Looking deeper into the transcriptomic data of the stem cell population (Dataset S1), we detected,
153 in addition to the well-known pituitary stem cell markers (*Sox2*, *Sox9*, *Cdh1*, *Krt8*, *Krt18*; *SI*
154 *Appendix*, Fig. S2D; (19)), a number of interesting genes which we validated by *in situ*
155 immunostaining analysis. *Tacstd2* (alias *Trop2*), found in stem cells of certain other tissues (24,
156 25), is within the AP stem cell population particularly expressed in SC1 (Dataset S1 and *SI*
157 *Appendix*, Fig. S2G). *In situ*, TACSTD2/TROP2 protein expression was observed in the cleft-
158 lining MZ stem cell compartment where it coincides with SOX2 (*SI Appendix*, Fig. S2G).
159 Interestingly, TACSTD2 was not detected in the SOX2⁺ cell groups in the AP parenchyma (*SI*
160 *Appendix*, Fig. S2G), thereby providing an appealing marker to distinguish MZ from parenchymal
161 stem cells (1, 2, 7). Of note, *Tacstd2* is also observed in the corticotrope cell cluster (Dataset S1
162 and *SI Appendix*, Fig. S2G). In agreement, TACSTD2 protein was detected in certain ACTH⁺
163 cells, mainly located at the transition area between AP and IL (the so-called 'wedges'; (26)) (*SI*
164 *Appendix*, Fig. S2G). Furthermore, the core Hippo pathway component *Yap1* was found highly
165 expressed in the stem cell population (both SC1 and SC2; Dataset S1 and *SI Appendix*, Fig.
166 S2H). In analogy, nuclear YAP⁺ signal is present in SOX2⁺ stem cells (both in the MZ and
167 parenchyma) (*SI Appendix*, Fig. S2H), thereby expanding our previous findings (14) and
168 confirming former studies that identified Hippo pathway activity in pituitary stem cells as
169 particularly studied during embryonic and neonatal development (27, 28). *Yap1* expression is also
170 seen in the connective tissue cluster, and in the endothelial cell clusters (Dataset S1 and *SI*
171 *Appendix*, Fig. S2H) which is consistent with YAP reported in pituitary endothelial cells (27).

172 Finally, our scRNA-seq exploration revealed high and specific expression of *Cyp2f2* in the
173 pituitary stem cell population (both SC1 and SC2; Dataset S1 and *SI Appendix*, Fig. S2I), in
174 agreement with another recent pituitary scRNA-seq study (21). Here, we validated this expression
175 and found that CYP2F2 is indeed localized in SOX2⁺ stem cells (*SI Appendix*, Fig. S2I).

176 As described above, the pituitary stem cell population acutely reacts to local tissue damage,
177 predominantly in the young gland. To search for molecular mechanisms underlying this acute
178 injury response, we contrasted the stem cell transcriptomes of young damaged AP with
179 undamaged gland using differentially expressed gene (DEG) and gene ontology (GO) analyses.
180 Among the top DEGs, we found multiple inflammatory-related genes (e.g. *Cxcl10*, *Ifi272a*, *Ifitm3*,
181 *Il6*, *Lcn2*, *Socs3*) that were upregulated following injury (Fig. 2D,E and Dataset S2). Accordingly,
182 cytokine-/inflammatory response-related GO terms were enriched in the stem cell clusters upon
183 damage (Fig. 2F and Dataset S3). Interestingly, within this context, the cytokine interleukin-6 (*Il6*)
184 was found highly upregulated, particularly in subcluster SC1 (Fig. 2D,E,G and Dataset S2). *Il6*
185 upregulation was also readily detected by RT-qPCR analysis in damaged *versus* undamaged AP
186 (*SI Appendix*, Fig. S2J). Further scRNA-seq scrutiny showed that *Il6* expression is not only
187 present in SC1, but also in the connective tissue cluster in which it also rises upon damage (Fig.
188 2G and Dataset S2). To validate the scRNA-seq expression pattern, we performed RNAscope *in*
189 *situ* hybridization for *Il6*, *Sox2* and *S100a6*, a gene highly expressed in both stem cell and
190 connective tissue clusters (Dataset S1 and *SI Appendix*, Fig. S2K). This *in situ* examination
191 showed cellular overlap of the mRNA signals (Fig. 2G). Both stem cell and connective
192 (supportive) tissue cells belong to the so-called folliculostellate (FS) cell group of the pituitary, a
193 heterogeneous cell population in the past designated as local IL-6 source, and in rat marked by
194 S100β (29–31). In analogy, S100A6 immunoreactivity is found in SOX2⁺ stem cells of mouse
195 pituitary, as well as in some non-SOX2⁺ cells (*SI Appendix*, Fig. S2K). Finally, *Il6* gene
196 expression is also detected in the endothelial cell population by scRNA-seq mining (Fig. 2G and
197 Dataset S1), *in situ* also supported by RNAscope analysis showing *Il6* signal in a number of cells
198 expressing the endothelial cell-specific plasmalemma vesicle associated protein (*Plvap*) (*SI*
199 *Appendix*, Fig. S2L).

200

201

202

203 **Interleukin-6 acts as a pituitary stem cell-activating factor at young age**

204 Since IL-6 has been shown to activate stem cells in certain other tissues when upregulated upon
205 local damage (such as in muscle and intestine; (32–34)), we addressed the question whether the
206 cytokine may also act as pituitary stem cell-activating factor.

207 Adding IL-6 to organoid culture augments organoid formation efficiency from undamaged (young)
208 AP (Fig. 3A), concomitant with proliferative activation of the organoid-driving stem cells (as
209 analyzed by EdU incorporation; Fig. 3B). In contrast, IL-6 does not further enhance organoid
210 formation from the damaged (young) gland (Fig. 3A) in which the stem cells are already activated
211 and endogenous IL-6 levels elevated (see above; and as observed in the supernatant of starting
212 organoid cultures (P0, day 3 of culture); Fig 3C).

213 The JAK/STAT pathway is a key downstream mediator of IL-6 signaling (35). IL-6 indeed
214 augments the number of phosphorylated STAT3 (phospho-STAT3 or pSTAT3)-immunopositive
215 cells in organoids from undamaged (young) AP, but not from damaged gland in which the
216 pSTAT3⁺ status is already high without IL-6 (Fig. 3D), advocating that the JAK/STAT pathway is
217 activated in stem cells following the DT-induced tissue injury, as also supported by intense *Stat3*
218 regulon activity in the damaged AP SC1 (*SI Appendix*, Fig S3A). Adding the STAT3 inhibitor
219 STATTIC to AP cells from damaged gland largely blocks organoid formation indicating the
220 importance of JAK/STAT signaling in this stem cell-driven process (Fig. 3E). Furthermore,
221 supplementation of LMT-28, an antagonist of the IL-6 co-receptor gp130 (36), abolishes organoid
222 formation (Fig. 3E). Along the same line, adding STATTIC and LMT-28 to undamaged AP cells
223 counteracts the formation of organoids, with the stimulatory effect of IL-6 no longer being
224 observed (Fig. 3E). Exposure of fully-grown organoids to LMT-28 results in a decrease in
225 pSTAT3⁺ cells and proliferative activity, and an increase in apoptosis (as analyzed by cleaved
226 caspase 3 or CC3 immunostaining; *SI Appendix*, Fig. S3B), supporting that gp130/pSTAT3-
227 mediated signaling is needed for stem cell proliferation and survival in the organoids. Taken

228 together, organoid read-out scrutiny indicates that IL-6 can act as pituitary stem cell activator and
229 reveals the importance of the IL-6-associated JAK/STAT and gp130 signaling pathways in
230 pituitary stem cell behavior.

231 To inspect whether IL-6 acts similarly *in vivo*, young WT mice were intraperitoneally (i.p.) injected
232 with the cytokine and the effect on pituitary stem cell-proliferative activity analyzed. The
233 proportion of proliferating SOX2⁺ stem cells is significantly elevated following IL-6 treatment,
234 concomitant with an increase in pSTAT3⁺ cells in the SOX2⁺ cell population (Fig. 3F), together
235 convincingly extrapolating the *in vitro* organoid-based findings to *in vivo*. Moreover, IL-6 injection
236 generated a pituitary stem cell activation response in IL-6 knockout (KO; IL-6^{-/-}) mice, whereas a
237 general inflammatory condition (as induced by CpG oligodeoxynucleotide (CpG) injection; (37))
238 did not (*SI Appendix*, Fig. S3C), demonstrating the specificity of the effect by IL-6 (independent of
239 a general inflammatory reaction if any). Of note, CpG-induced inflammation in WT mice triggers a
240 pituitary stem cell-proliferative reaction comparable to IL-6 (*SI Appendix*, Fig. S3C), in line with
241 the upregulated systemic IL-6 levels as reported to occur in this model (37). Intriguingly, the
242 SOX2⁺ stem cell population is not different in the IL-6 KO pituitary regarding number and
243 quiescent (low-proliferative) status (*SI Appendix*, Fig. S3D). However, primary organoid formation
244 from IL-6 KO AP is reduced (*versus* WT AP), and IL-6 KO organoids are not passagable (*SI*
245 *Appendix*, Fig. S3E), indicating that endogenous IL-6 is important for these stem cell activities.

246 Finally, to determine whether IL-6, being upregulated in the pituitary after damage, is involved in
247 the injury-induced stem cell activation, we applied anti-IL-6 antibody during the acute DT-
248 triggered damage infliction in GHC*re*/iDTR mice (Fig. 3G). The stem cell-proliferative reaction is
249 significantly reduced (Fig. 3G), coinciding with lowered pSTAT3⁺ cells in the AP (*SI Appendix*,
250 Fig. S3F). Similarly, *in vivo* LMT-28 administration during damage infliction reduces the proportion
251 of proliferating stem cells and pSTAT3⁺ cells in the AP (*SI Appendix*, Fig. S3G).

252 Taken all together, our data show that IL-6 is upregulated in young pituitary upon tissue damage
253 and can act as pituitary stem cell-activating factor. In addition, they provide evidence that IL-6 is
254 involved in the early stem cell activation reaction to injury.

255 **IL-6 does not activate stem cells in the aging pituitary, which is typified by an elevated**
256 **IL-6/inflammatory phenotype**

257 In clear contrast to the observations in young mice, i.p. injection of IL-6 in aging animals does not
258 trigger a stem cell-proliferative activation response (Fig. 4A). Intriguingly, basal *Il6* expression
259 level was found higher in aging *versus* young (undamaged) AP (Fig. 4B), in particular in the stem
260 cell subcluster SC1 (Fig. 4C and Dataset S4). DEG and GO analysis of the stem cell
261 transcriptomes identified upregulation of cytokine-/inflammatory response-related terms and
262 genes in the aging *versus* young (undamaged) pituitary SC1 (Fig. 4C-E and Dataset S3-4), and
263 even more broadly in the whole AP (Fig. 4E and Dataset S3-4). In analogy, gene set enrichment
264 analysis (GSEA) applied to the single-cell transcriptomic dataset revealed a striking enrichment of
265 the 'inflammatory response' hallmark in aging *versus* young (undamaged) AP, and in particular
266 also in its SC1 (Fig. 4F). Also, the 'IL-6/JAK/STAT3 signaling' hallmark is significantly enriched in
267 aging *versus* young AP and stem cell population (Fig. 4F). In accordance, pSTAT3⁺ cells are
268 more abundant in the aging pituitary (*SI Appendix*, Fig. S4A). Together, these findings indicate
269 that the aging pituitary, including its stem cells, displays a basally higher IL-6/inflammatory status
270 than the young gland, which may explain the absence of a stem-cell activation reaction in the
271 older AP upon IL-6 administration (see Fig. 4A), and the inferior stem cell reaction to injury (see
272 Fig. 1A). In support, injection of IL-6 does not further elevate the number of pSTAT3⁺ cells in the
273 aging gland (*SI Appendix*, Fig. S4B). Moreover, inflicting pituitary damage in aging mice does not
274 significantly increase *Il6* expression levels any further in the gland (*SI Appendix*, Fig. S4C) or its
275 SC1 and connective tissue cluster (Dataset S5 and *SI Appendix*, Fig. S4D). A raised
276 inflammatory nature at aging has also been found to occur in other organs, epitomized in the
277 concept of inflammaging which states that a chronic low-grade inflammation gradually develops
278 at progressing age, not only at the systemic but also organ level (38, 39), proposed to underlie
279 deteriorating organ and stem cell functionality at aging (40–43). Regarding systemic signs of
280 inflammaging, increased IL-6 level is the most clear and supported marker (38, 39). In
281 agreement, we found significantly upregulated IL-6 plasma levels in aging mice when compared
282 to young animals (Fig. 4G). Numbers of immune cells in the pituitary, encompassing resident and

283 infiltrated cells, are not altered in the aging animals (*SI Appendix*, Fig. S4E), similar to findings in
284 the spleen (*SI Appendix*, Fig. S4F), thereby suggesting that the inflammaging process may still be
285 subtle in the middle-aged (~1-year-old) animals when compared to elderly mice (~2 years) in
286 which macrophage infiltration has been reported in certain organs (44, 45). Along the same line,
287 plasma levels of (pro-)inflammatory cytokines other than IL-6, of which specifically TNF- α has
288 been reported to be upregulated in elderly mice in some studies (38, 39), are not significantly
289 changed (yet) in the middle-aged mice analyzed here (*SI Appendix*, Fig. S4G).

290 Taken together, our findings provide evidence that aging pituitary displays a raised
291 IL-6/inflammatory phenotype which may underlie the declined stem cell activation upon injury or
292 IL-6 exposure at aging.

293 **Activatability of aging pituitary stem cells re-surfaces in organoid culture**

294 Unexpectedly, in contrast to the absence of a stem cell-activating effect by IL-6 in the aging gland
295 *in vivo* (Fig. 4A), we observed that IL-6 is able to increase the formation and proliferative activity
296 of organoids from aging (undamaged) pituitary *in vitro* (Fig. 5A-B), concomitant with an elevation
297 of pSTAT3⁺ cells (*SI Appendix*, Fig. S5A). We hypothesized that the elevated inflammatory status
298 may swiftly disappear in culture when the stem cells are released from their old *in vivo*
299 (micro-)environment. In support, as opposed to the upregulated IL-6/inflammatory response
300 genes and hallmarks in aging pituitary and its stem cell clusters (see Fig. 4E-F and Dataset S3-
301 4), expression of *Il6* and inflammatory response genes is not different anymore between aging
302 and young pituitary stem cells once cultured *in vitro* in organoid conditions (analyzed at day 14 of
303 P0 organoid culture; Fig. 5C).

304 Finally, in view of its pituitary stem cell-activating competence and importance for organoid
305 culture as found in IL-6 KO conditions, we tested whether addition of IL-6 to organoid cultures
306 prolongs their yet limited expandability (19). Indeed, administration of IL-6 significantly increased
307 organoid passageability, from both young and aging, damaged and undamaged pituitary (Fig.
308 5D). Endogenous IL-6 expression and production was found to substantially decline during
309 organoid culturing in subsequent passages (Fig. 5E; *SI Appendix*, Fig. S5B), plausibly underlying
310 the before limited expandability in the absence of exogenous IL-6 supplementation. After long-

311 term passaging, organoids maintain their morphological and pituitary stem cell phenotype (as
312 shown for damaged AP; *SI Appendix, Fig. S5C*).

313 Taken together, the aging pituitary's stem cells retain intrinsic activation capability which re-
314 surfaces *in vitro* when liberated from the plausibly impeding IL-6/inflammatory stress *in vivo*.
315 Moreover, achieving robust long-term expansion empowers the applicability of the organoid
316 model system toward extensive exploration of pituitary stem cell biology and activation.

317 **Discussion**

318 In the present study, we searched for molecular mechanisms underlying the acute activation of
319 adult pituitary stem cells upon local tissue injury, at present entirely unknown, and looked for
320 differences with the aging gland, reported before to have lost damage-repair capacity (14). By
321 applying single-cell transcriptomic profiling, we tracked down IL-6 as a factor that has the capacity
322 to bring pituitary stem cells into activation mode. Back in 1989, we made the intriguing
323 observation that a cytokine known for expression and function in the immune system (i.e. IL-6)
324 was also expressed in an endocrine organ (i.e. the pituitary gland) (30, 46). IL-6 was found to be
325 produced by the so-called FS cell population which represents a yet ill-defined, heterogeneous
326 cell-type assembly in the pituitary, proposed to encompass paracrine-regulatory cells, physically
327 supportive (connective tissue) cells, immune-associated cells and more recently, also stem cells
328 (1, 2, 29, 31). Now 30 years later, our scRNA-seq interrogation eventually confirmed and refined
329 the pituitary IL-6 source. The upregulation of IL-6 upon injury in the young gland, occurring
330 particularly in the stem cell and connective tissue subsets, proposes a role, paracrine and/or
331 autocrine, for these specific cell subpopulations in the injury-triggered stem cell activation
332 (summarized in *SI Appendix, Fig. S5D*). *In vitro*, IL-6 was found to activate the pituitary stem cells
333 resulting in more efficient organoid development, a newly developed tool to probe pituitary stem
334 cell biology and activation (19). *In vivo*, IL-6 triggered acute pituitary stem cell activation in the
335 young gland while blockade of IL-6 or associated signaling pathways strongly reduced the stem
336 cell reaction at injury, together providing evidence that IL-6 is involved in the acute activation
337 process of the quiescent pituitary stem cells in response to local tissue damage. Of note, IL-6
338 does not seem to be involved in the stem cell phenotype of the homeostatic gland which is not

339 changed in IL-6 KO mice, not illogical given the highly quiescent state of the stem cells in the
340 basal gland, not in need of IL-6 action. It should be remarked that damage still induced some
341 proliferative stem cell activation in the aging pituitary *in vivo* while IL-6 injection did not (Fig. 1A
342 and Fig. 4A), and that the proliferative activation reached in young mice after damage appeared
343 higher than after IL-6 injection (Fig. 1A and Fig. 3F). One explanation may be that local IL-6 levels
344 in young pituitary after damage are higher than achieved after i.p. IL-6 injection. Furthermore, still
345 other factors may additionally be involved in the stem cell activation process after injury (S/
346 Appendix, Fig. S5D). Our scRNA-seq resource now provides an invaluable means to in-depth
347 elucidate this molecular machinery, including the search for the upstream activators of IL-6
348 expression during damage.

349 Excitingly, our study demonstrates that the stem cells of aging pituitary regain activatability when
350 removed from their *in vivo* tissue milieu. Hence, receded *in vivo* responsiveness and reaction to
351 injury is not an intrinsic aging process of the pituitary stem cells, but may rather be imposed by an
352 oppressive (inflammatory) microenvironment. Also in certain other tissues, it has been shown that
353 stem cells retain their functional capacities at aging which is repressed by the environment (16–
354 18, 47). Substituting the old milieu for a younger equivalent restored stem cell functionality in
355 these tissues (18, 38, 47, 48). Taken together, we advance the concept (as summarized in S/
356 Appendix, Fig. S5D) that the raised inflammatory environment in the aging pituitary, indicative of
357 inflammaging, presents a roadblock for full activation of the resident stem cells upon injury. Or in
358 other words, the prevailing IL-6/inflammatory milieu in the aging pituitary sets a threshold that is
359 hard to surpass for unfolding an adequate acute reaction when challenged by injury. In the end,
360 the subsided acute reaction of the stem cells may contribute to the absence of the later
361 regeneration in aging pituitary upon cell-ablation injury (14). Indeed, it has been reported in other
362 tissues that acute activation of the resident stem cells by IL-6 following insult represents a first
363 essential step toward eventual repair (34, 49, 50). Definite evidence for an *in vivo* role of IL-6 in
364 eventual pituitary regeneration awaits extensive and comprehensive scrutiny of GHC*Cre*/iDTR
365 mice on the IL-6 KO background, ideally in a conditional (temporospatial), pituitary
366 (stem/connective cell)-specific manner. Interestingly, it has been found that anti-inflammatory

367 intervention can restore regenerative capacity at aging in certain tissues (such as skin, muscle,
368 liver, gut; (40–43)), an appealing path for future pituitary aging research. Finally, the present
369 study strongly enlarges the applicability of our recently developed pituitary organoid model by
370 effectively extending organoid expandability using IL-6, thus compensating for the decline of
371 endogenous IL-6 production, which could be due to the disappearance of *in situ* stimulatory
372 factors.

373 In conclusion, we identified and characterized IL-6 as pituitary stem cell activator, a competence
374 quenched at aging concurrent with a raised IL-6/inflammatory stress level in the gland. Still, aging
375 pituitary stem cells retain intrinsic stemness properties and show activatability when released
376 from their *in vivo* microenvironment. These new insights may be instrumental to find strategies for
377 restraining the master endocrine pituitary gland from aging, or for rejuvenating a burdened old
378 gland. And more in general, our single-cell transcriptome database provides a rich source to
379 search for processes underlying pituitary aging whose understanding is currently poor, and for
380 potential therapeutic targets. In the end, IL-6 and inflammaging may represent appealing
381 candidates.

382 **Methods**

383 **Mice and *in vivo* treatments**

384 GHC*re*/iDTR and control (-iDTR) mice were injected with DT, and pituitaries (damaged and
385 undamaged, respectively) collected (Fig. 2A). Young and/or aging mice were treated with IL-6,
386 anti-IL-6 antibody, CpG or LMT-28 according to the indicated or described schedules. Further
387 details are provided in *SI Appendix*.

388 **Single-cell RNA sequencing**

389 Damaged and undamaged AP from young and aging mice were dissociated into single cells (51,
390 52) and subjected to scRNA-seq analyses using 10x Genomics (Fig. 2A), according to
391 manufacturer instructions. Libraries were sequenced and downstream analysis was performed in
392 R using Seurat (53). Gene regulatory networks (regulons) were determined using SCENIC (22) in
393 Python (pySCENIC). More details are given in *SI Appendix*.

394 **Pituitary organoids**

395 AP cells were plated in a drop of 70% Matrigel/30% serum-free defined medium (SFDM; Thermo
396 Fisher Scientific), and pituitary organoid culture medium (19) was added. After growth (10-14
397 days), organoids were dissociated into small fragments which were re-seeded in Matrigel drops
398 for passaging. More details are provided in *SI Appendix*.

399 **Immunostaining**

400 Whole pituitary and organoids were fixed and sections subjected to immunofluorescence staining
401 (for antibodies, see *SI Appendix*, Table S1), or to transmission electron microscopy (see *SI*
402 *Appendix*). Immunopositive-cell quantification and EdU labelling in organoids are described in *SI*
403 *Appendix*.

404 **RNAscope *in situ* hybridization**

405 Whole pituitary was fixed and sections subjected to RNAscope analysis according to the
406 manufacturer's recommendations (Advanced Cell Diagnostics). More details are provided in *SI*
407 *Appendix*.

408 **Gene expression analysis by RT-qPCR**

409 RNA was reverse-transcribed (RT) and subjected to quantitative real-time PCR (qPCR) as
410 previously described (19) using primers as listed in *SI Appendix*, Table S2. Further details are
411 given in *SI Appendix*.

412 **IL-6 measurement**

413 IL-6 concentration was measured in organoid culture supernatant and mouse plasma using MSD
414 (Meso Scale Discovery) kits according to the manufacturer's protocol (see *SI Appendix*).

415 **Statistical analysis**

416 Statistical analysis was performed using GraphPad Prism, as in detail described in *SI Appendix*.
417 Statistical significance was defined as $P \leq 0.05$.

418 **Acknowledgments**

419 We thank Y. Van Goethem and V. Vanslembrouck for valuable technical help. We thank the VIB
420 Nucleomics Core (in particular Rekin's Janky) and KU Leuven Genomics Core (particularly Álvaro
421 Cortés Calabuig) for their expert assistance in scRNA-seq analysis, as well as Thomas Van
422 Brussel and Bram Boeckx (D. Lambrechts' group, KU Leuven) for technical and bioinformatical
423 support in scRNA-seq experiments, respectively. The computational resources used for scRNA-
424 seq analysis were provided by the 'Vlaams Supercomputer Centrum' (VSC), managed by the
425 'Fonds Wetenschappelijk Onderzoek (FWO) – Vlaanderen'. We are also grateful to the Imaging
426 Core (VIB, KU Leuven) and the Cell and Tissue Imaging Cluster (CIC; KU Leuven) for the use of
427 microscopes, and the Center for Brain & Disease Research (CBD) Histology unit (VIB, KU
428 Leuven) for the use of histology equipment. We acknowledge the use of the Electron Microscopy
429 Platform (VIB, KU Leuven) and the Institute of Development, Aging and Cancer (Tohoku
430 University, Sendai, Japan) for transmission electron microscopy.

431 **Funding**

432 This work was supported by several grants from the 'Bijzonder Onderzoeksfonds' (BOF) KU
433 Leuven and from FWO – Vlaanderen, awarded to the principal investigators. A.V. (1141717N),
434 E.L. (11A3320N), B.C. (11W9215N), A.J. (1158318N) and C.N. (1S14218N) are supported by a
435 PhD Fellowship from the FWO/FWO-SB.

436 **Competing financial interests**

437 The authors declare no competing financial interests.

438 **References**

- 439 1. T. Fauquier, K. Rizzoti, M. Dattani, R. Lovell-Badge, I. C. A. F. Robinson, SOX2-
440 expressing progenitor cells generate all of the major cell types in the adult mouse pituitary
441 gland. *Proceedings of the National Academy of Sciences of the United States of America*
442 **105**, 2907–12 (2008).
- 443 2. J. Chen, *et al.*, Pituitary progenitor cells tracked down by side population dissection. *Stem*
444 *Cells* **27**, 1182–1195 (2009).
- 445 3. K. Rizzoti, H. Akiyama, R. Lovell-Badge, Mobilized adult pituitary stem cells contribute to
446 endocrine regeneration in response to physiological demand. *Cell Stem Cell* **13**, 419–432
447 (2013).

- 448 4. C. L. Andoniadou, *et al.*, Sox2+ stem/progenitor cells in the adult mouse pituitary support
449 organ homeostasis and have tumor-inducing potential. *Cell Stem Cell* **13**, 433–445 (2013).
- 450 5. H. Vankelecom, J. Chen, Pituitary stem cells: Where do we stand? *Molecular and Cellular*
451 *Endocrinology* **385**, 2–17 (2014).
- 452 6. B. Cox, H. Roose, A. Vennekens, H. Vankelecom, Pituitary stem cell regulation: Who is
453 pulling the strings? *Journal of Endocrinology* **234**, R135–R158 (2017).
- 454 7. H. Vankelecom, “Pituitary stem cells: Quest for hidden functions” in *Stem Cells in*
455 *Neuroendocrinology*, D. Pfaff, Y. Christen, Eds. (Springer International Publishing, 2016),
456 pp. 81–101.
- 457 8. X. Zhu, J. Tollkuhn, H. Taylor, M. G. Rosenfeld, Notch-dependent pituitary SOX2+ stem
458 cells exhibit a timed functional extinction in regulation of the postnatal gland. *Stem Cell*
459 *Reports* **5**, 1196–1209 (2015).
- 460 9. H. Roose, *et al.*, Major depletion of SOX2+ stem cells in the adult pituitary is not restored
461 which does not affect hormonal cell homeostasis and remodelling. *Scientific Reports* **7**, 1–
462 11 (2017).
- 463 10. A. S. Brack, T. A. Rando, Tissue-specific stem cells: Lessons from the skeletal muscle
464 satellite cell. *Cell Stem Cell* **10**, 504–514 (2012).
- 465 11. A. Miyajima, M. Tanaka, T. Itoh, Stem/progenitor cells in liver development, homeostasis,
466 regeneration, and reprogramming. *Cell Stem Cell* **14**, 561–574 (2014).
- 467 12. Q. Fu, *et al.*, The adult pituitary shows stem/progenitor cell activation in response to injury
468 and is capable of regeneration. *Endocrinology* **153**, 3224–35 (2012).
- 469 13. Q. Fu, H. Vankelecom, Regenerative capacity of the adult pituitary: multiple mechanisms
470 of lactotrope restoration after transgenic ablation. *Stem Cells and Development* **21**, 3245–
471 57 (2012).
- 472 14. C. Willems, *et al.*, Regeneration in the pituitary after cell-ablation injury : time-related
473 aspects and molecular analysis. *Endocrinology* **157**, 705–721 (2016).
- 474 15. D. J. Rossi, *et al.*, Cell intrinsic alterations underlie hematopoietic stem cell aging.
475 *Proceedings of the National Academy of Sciences of the United States of America* **102**,
476 9194–9199 (2005).
- 477 16. M. B. Schultz, D. A. Sinclair, When stem cells grow old: Phenotypes and mechanisms of
478 stem cell aging. *Development (Cambridge)* **143**, 3–14 (2016).
- 479 17. C. Domingues-Faria, M. P. Vasson, N. Goncalves-Mendes, Y. Boirie, S. Walrand,
480 Skeletal muscle regeneration and impact of aging and nutrition. *Ageing Research Reviews*
481 **26**, 22–36 (2016).
- 482 18. M. Segel, *et al.*, Niche stiffness underlies the ageing of central nervous system progenitor
483 cells. *Nature* **573**, 130–134 (2019).
- 484 19. B. Cox, *et al.*, Organoids from pituitary as a novel research model toward pituitary stem
485 cell exploration. *Journal of Endocrinology* **240**, 287–308 (2019).
- 486 20. L. McInnes, J. Healy, J. Melville, UMAP: Uniform manifold approximation and projection
487 for dimension reduction (2018).
- 488 21. L. Y. M. Cheung, *et al.*, Single-cell RNA sequencing reveals novel markers of male
489 pituitary stem cells and hormone-producing cell types. *Endocrinology* **159**, 3910–3924
490 (2018).
- 491 22. S. Aibar, *et al.*, SCENIC: Single-cell regulatory network inference and clustering. *Nature*
492 *Methods* **14**, 1083–1086 (2017).
- 493 23. A. Mayran, *et al.*, Pioneer and nonpioneer factor cooperation drives lineage specific
494 chromatin opening. *Nature Communications* **10**, 3807 (2019).
- 495 24. V. Fernandez Vallone, *et al.*, Trop2 marks transient gastric fetal epithelium and adult
496 regenerating cells after epithelial damage. *Development* **143**, 1452–1463 (2016).
- 497 25. A. S. Goldstein, *et al.*, Trop2 identifies a subpopulation of murine and human prostate
498 basal cells with stem cell characteristics. *Proceedings of the National Academy of*
499 *Sciences of the United States of America* **105**, 20882–20887 (2008).
- 500 26. L. Gremaux, Q. Fu, J. Chen, H. Vankelecom, Activated phenotype of the pituitary
501 stem/progenitor cell compartment during the early-postnatal maturation phase of the
502 gland. *Stem Cells and Development* **21**, 801–13 (2012).

- 503 27. E. J. Lodge, J. P. Russell, A. L. Patist, P. Francis-West, C. L. Andoniadou, Expression
504 analysis of the Hippo cascade indicates a role in pituitary stem cell development. *Frontiers*
505 *in Physiology* **7**, 1–11 (2016).
- 506 28. E. J. Lodge, *et al.*, Homeostatic and tumorigenic activity of SOX2+ pituitary stem cells is
507 controlled by the LATS/YAP/TAZ cascade. *eLife* **8**, 1–26 (2019).
- 508 29. H. Vankelecom, Pituitary stem cells drop their mask. *Current Stem Cell Research &*
509 *Therapy* **7**, 36–71 (2012).
- 510 30. H. Vankelecom, P. Carmeliet, J. van Damme, A. Billiau, C. Deneef, Production of
511 interleukin-6 by folliculo-stellate cells of the anterior pituitary gland in a histiotypic cell
512 aggregate culture system. *Neuroendocrinology* **49**, 102–106 (1989).
- 513 31. W. Allaerts, H. Vankelecom, History and perspectives of pituitary folliculo-stellate cell
514 research. *European Journal of Endocrinology* **153**, 1–12 (2005).
- 515 32. A. L. Serrano, B. Baeza-Raja, E. Perdiguero, M. Jardí, P. Muñoz-Cánoves, Interleukin-6
516 is an essential regulator of satellite cell-mediated skeletal muscle hypertrophy. *Cell*
517 *Metabolism* **7**, 33–44 (2008).
- 518 33. P. Muñoz-Cánoves, C. Scheele, B. K. Pedersen, A. L. Serrano, Interleukin-6 myokine
519 signaling in skeletal muscle: A double-edged sword? *FEBS Journal* **280**, 4131–4148
520 (2013).
- 521 34. K. A. Kuhn, N. A. Manieri, T. C. Liu, T. S. Stappenbeck, IL-6 stimulates intestinal
522 epithelial proliferation and repair after injury. *PLoS ONE* **9**, 1–18 (2014).
- 523 35. S. Rose-John, Interleukin-6 family cytokines. *Cold Spring Harbor Perspectives in Biology*
524 **10**, 1–18 (2018).
- 525 36. S.-S. Hong, *et al.*, A novel small-molecule inhibitor targeting the IL-6 receptor β subunit,
526 glycoprotein 130. *The Journal of Immunology* **195**, 237–245 (2015).
- 527 37. E. Behrens, *et al.*, Repeated TLR9 stimulation results in macrophage activation syndrome
528 like disease in mice. *Journal of Clinical Investigation* **121**, 2264–2277 (2011).
- 529 38. C. Franceschi, J. Campisi, Chronic inflammation (Inflammaging) and its potential
530 contribution to age-associated diseases. *Journals of Gerontology - Series A Biological*
531 *Sciences and Medical Sciences* **69**, S4–S9 (2014).
- 532 39. C. Franceschi, *et al.*, Inflamm-aging: An evolutionary perspective on immunosenescence.
533 *Annals of the New York Academy of Sciences* **908**, 244–254 (2000).
- 534 40. J. Neves, P. Sousa-Victor, Regulation of inflammation as an anti-aging intervention.
535 *FEBS Journal* **287**, 43–52 (2020).
- 536 41. J. Oh, *et al.*, Age-associated NF- κ B signaling in myofibers alters the satellite cell niche
537 and re-strains muscle stem cell function. *Aging* **8**, 2871–2896 (2016).
- 538 42. D. Jurk, *et al.*, Chronic inflammation induces telomere dysfunction and accelerates
539 ageing in mice. *Nature Communications* **2** (2014).
- 540 43. J. Doles, M. Storer, L. Cozzuto, G. Roma, W. M. Keyes, Age-associated inflammation
541 inhibits epidermal stem cell function. *Genes and Development* **26**, 2144–2153 (2012).
- 542 44. R. Büttner, *et al.*, Inflammaging impairs peripheral nerve maintenance and regeneration.
543 *Aging Cell* **17** (2018).
- 544 45. R. Lu, N. K. Sampathkumar, B. A. Benayoun, “Measuring phagocytosis in bone marrow-
545 derived macrophages and peritoneal macrophages with aging” in *Physiology & Behavior*,
546 (2020), pp. 161–170.
- 547 46. H. Vankelecom, *et al.*, Immunocytochemical evidence that S-100-positive cells of the
548 mouse anterior pituitary contain interleukin-6 immunoreactivity. *Journal of Histochemistry*
549 *and Cytochemistry* **41**, 151–156 (1993).
- 550 47. I. M. Conboy, *et al.*, Rejuvenation of aged progenitor cells by exposure to a young
551 systemic environment. *Nature* **433**, 760–764 (2005).
- 552 48. A. S. I. Ahmed, M. H. Sheng, S. Wasnik, D. J. Baylink, K.-H. W. Lau, Effect of aging on
553 stem cells. *World Journal of Experimental Medicine* **7**, 1 (2017).
- 554 49. E. Galun, S. Rose-John, “The regenerative activity of Interleukin-6” in *Tissue-Protective*
555 *Cytokines: Methods and Protocols*, (2013), pp. 59–77.
- 556 50. T. Tadokoro, *et al.*, IL-6/STAT3 promotes regeneration of airway ciliated cells from basal
557 stem cells. *Proceedings of the National Academy of Sciences of the United States of*
558 *America* **111**, 3641–3649 (2014).

- 559 51. C. Denef, E. Hautekeete, A. de Wolf, B. Vanderschueren, Pituitary basophils from
560 immature male and female rats: distribution of gonadotrophs and thyrotrophs as studied
561 by unit gravity sedimentation. *Endocrinology* **103**, 724–735 (1978).
562 52. B. van der Schueren, C. Denef, J.-J. Cassiman, Ultrastructural and functional
563 characteristics of rat pituitary cell aggregates. *Endocrinology* **110**, 513–523 (1982).
564 53. A. Butler, P. Hoffman, P. Smibert, E. Papalexi, R. Satija, Integrating single-cell
565 transcriptomic data across different conditions, technologies, and species. *Nature*
566 *Biotechnology* **36**, 411–420 (2018).
567
568

569 **Legends to Figures**

570 **Fig. 1.** Pituitary stem cell activation following tissue injury subsides at aging. (A)
571 Immunofluorescence staining of SOX2 (magenta) and Ki67 (green) in basal (undamaged) and
572 damaged anterior pituitary (AP)-derived cytopsin samples of young and aging mice. Nuclei are
573 labeled with Hoechst33342 (blue). Arrowheads indicate double-immunopositive cells. (Scale bar,
574 50 μm .) Bar graphs show the proportion of SOX2⁺Ki67⁺ cells in SOX2⁺ cells (mean \pm SEM), and
575 the fold change in absolute SOX2⁺Ki67⁺ cell number (mean \pm SEM) after damage (i.e. relative to
576 undamaged AP, set as 1 (dashed line)) (for calculation of absolute cell numbers, see Extended
577 Methods in *SI Appendix*). Data points represent biological replicates. * $P \leq 0.05$; ** $P \leq 0.01$; *** $P \leq$
578 0.001; **** $P \leq 0.0001$. (B) Organoid formation efficiency from undamaged and damaged, young
579 and aging AP. Representative bright-field pictures of organoid cultures are shown (passage 0,
580 P0; scale bar, 500 μm .) Bar graphs indicate number of organoids developed and fold change in
581 organoid number after pituitary damage (relative to undamaged AP) (mean \pm SEM). Data points
582 represent biological replicates. * $P \leq 0.05$; ** $P \leq 0.01$. (C) Percentage of organoid-initiating SOX2⁺
583 cells per well of 10,000 seeded AP cells from the conditions as indicated. Bar graphs show mean
584 \pm SEM and data points represent biological replicates. * $P \leq 0.05$.

585

586 **Fig. 2.** Single-cell transcriptomic profiling reveals upregulation of interleukin-6 in young pituitary
587 following tissue injury. (A) Experimental schematic for the scRNA-seq analysis. DT, diphtheria
588 toxin; AP, anterior pituitary; IL, intermediate lobe; PP, posterior pituitary. Mouse icon obtained
589 from freepik.com. (B) UMAP plot of the annotated cell clusters in the aggregate AP samples (i.e.
590 collective single-cell transcriptome datasets from young and aging, undamaged and damaged
591 AP). Somato, somatotropes; Lacto, lactotropes; Cortico, corticotropes; Gonado, gonadotropes;
592 Thyro, thyrotropes; Melano, melanotropes; SC1 and SC2, stem cell cluster 1 and 2; EC1 and
593 EC2, endothelial cell cluster 1 and 2; Immune, immune cells; CT, connective tissue cells;
594 Apoptotic, apoptotic cells. (C) UMAP plot of undamaged and damaged AP (young and aging
595 combined). (D) Heatmaps displaying the scaled expression of inflammatory response genes in
596 the stem cell clusters SC1 and SC2 of young undamaged and damaged AP. (E) Volcano plot

597 displaying DEGs in SC1 of young AP. Colored dots represent significantly up- (orange) and
598 down- (green) regulated genes in damaged *versus* undamaged AP. A selection of genes (as
599 mentioned in the text) is indicated, and interleukin-6 (Il6) is highlighted. (F) Significant (FDR \leq
600 0.05) DEG-associated GO terms linked with inflammatory processes enriched in SC1 and SC2 of
601 young damaged *versus* undamaged AP. (G) Violin plot (top) and projection on UMAP diagram
602 (bottom) of *Il6* expression in young undamaged and damaged AP with indication of relevant cell
603 clusters. Triple RNAscope *in situ* hybridization analysis of young (undamaged) AP for *Sox2*
604 (cyan), *Il6* (magenta) and *S100a6* (yellow). Boxed areas are magnified. Nuclei are stained with
605 DAPI (blue). Arrowheads indicate cells with colocalized expression. (Scale bar, 50 μm .)

606

607 **Fig. 3.** IL-6 acts as pituitary stem cell-activating factor at young age. (A) Organoid development
608 from undamaged and damaged young AP in the absence (control, CTRL) or presence of IL-6
609 (P0; scale bar, 500 μm .) Bar graphs show number of organoids formed (mean \pm SEM). Data
610 points represent biological replicates. $*P \leq 0.05$. (B) Proliferative activity of organoids grown in the
611 absence (CTRL) or presence of IL-6 (P0), as assessed by EdU incorporation (green). Nuclei are
612 stained with Hoechst33342 (blue). (Scale bar, 50 μm .) Bar graph shows percentage of EdU⁺ cells
613 in organoids (mean \pm SEM). Data points represent individual organoids from 3 biological
614 replicates. $****P \leq 0.0001$. (C) IL-6 protein levels in supernatant of organoid cultures (P0, day 3 of
615 culture) from young undamaged and damaged AP. Bar graph shows mean \pm SEM and data
616 points represent biological replicates. $*P \leq 0.05$. (D) Immunofluorescence staining of pSTAT3
617 (green) in young AP organoids grown in the absence (CTRL) or presence of IL-6 (P0). Nuclei are
618 stained with Hoechst33342 (blue). (Scale bar, 100 μm .) Bar graphs show percentage of pSTAT3⁺
619 cells in organoids (mean \pm SEM). Data points represent biological replicates. $**P \leq 0.01$. (E)
620 Organoid development from young damaged AP treated as indicated (P0; scale bar, 500 μm .)
621 Bar graphs show number of organoids formed (mean \pm SEM) from young damaged and
622 undamaged AP under conditions as indicated. Data points represent biological replicates. $*P \leq$
623 0.05. (F) Time schedule of *in vivo* treatment with IL-6. Immunofluorescence staining of SOX2
624 (magenta) and Ki67 (green) in basal (undamaged) AP-derived cytospin samples of young

625 wildtype (WT) mice, *in vivo* injected with IL-6 or vehicle (CTRL). Nuclei are labeled with
626 Hoechst33342 (blue). Arrowheads indicate double-immunopositive cells. (Scale bar, 50 μ m.) Bar
627 graphs show percentage of SOX2⁺Ki67⁺ or SOX2⁺pSTAT3⁺ cells in SOX2⁺ cells (mean \pm SEM)
628 and data points represent biological replicates. * $P \leq 0.05$. (G) Time schedule of *in vivo* treatment
629 with anti-IL-6 antibody (IL-6 Ab). Bar graph shows percent change (relative to CTRL with mean
630 set to 100%) of SOX2⁺Ki67⁺ cells in SOX2⁺ cells (determined using cytopsin samples) in the AP
631 of young mice subjected to DT-induced damage infliction, and simultaneously treated with IL-6 Ab
632 (mean \pm SEM). Data points represent biological replicates. * $P \leq 0.05$.

633

634 **Fig. 4.** IL-6 does not activate stem cells in aging pituitary which displays an elevated
635 IL-6/inflammatory phenotype. (A) Time schedule of *in vivo* treatment with IL-6.
636 Immunofluorescence staining of SOX2 (magenta) and Ki67 (green) in basal (undamaged) AP-
637 derived cytopsin samples of aging WT mice, *in vivo* injected with IL-6 or vehicle (CTRL). Nuclei
638 are labeled with Hoechst33342 (blue). Arrowheads indicate double-immunopositive cells. (Scale
639 bar, 50 μ m.) Bar graph shows percentage of SOX2⁺Ki67⁺ cells in SOX2⁺ cells (mean \pm SEM) and
640 data points represent biological replicates. (B) *Il6* gene expression in aging *versus* young basal
641 (undamaged) AP as determined by RT-qPCR. Bar graph shows fold change in aging AP relative
642 to young (mean \pm SEM) and data points represent biological replicates. ** $P \leq 0.01$. (C) Volcano
643 plot displaying DEGs in SC1 in young and aging undamaged AP. Colored dots represent
644 significantly up- (blue) and down- (pink) regulated genes in aging *versus* young AP. A selection of
645 genes is indicated, and *Il6* is highlighted. (D) Significant (FDR ≤ 0.05) DEG-associated GO terms
646 linked with inflammatory processes enriched in the stem cell cluster SC1 of aging *versus* young
647 (undamaged) AP. (E) Heatmap displaying the fold change (presented as $-\log_{10}FC$) of inflammatory
648 response genes up- (blue) and down- (pink) regulated at aging. (F) GSEA analysis of
649 'inflammatory response' and 'IL-6/JAK/STAT3' hallmarks in aging compared to young
650 (undamaged) AP and its SC1 and SC2, visualized as normalized enrichment score (NES). **FDR
651 ≤ 0.01 ; ****FDR ≤ 0.0001 ; ns, non-significant. (G) Systemic plasma levels of IL-6 in young and

652 aging WT (undamaged) mice. Bar graph shows mean \pm SEM, and data points represent
653 biological replicates. $*P \leq 0.05$.

654 **Fig. 5.** Aging pituitary's stem cells regain activatability to IL-6 in organoid culture. (A) Organoid
655 development from undamaged and damaged aging AP in the absence (CTRL) or presence of IL-
656 6 (P0; scale bar, 500 μm .) Bar graphs show number of organoids formed (mean \pm SEM). Data
657 points represent biological replicates. $*P \leq 0.05$. (B) Proliferative activity of organoids grown in the
658 absence (CTRL) or presence of IL-6 (P0), as assessed by EdU incorporation (green). Nuclei are
659 stained with Hoechst33342 (blue). (Scale bar, 50 μm .) Bar graph shows percentage of EdU⁺ cells
660 in organoids (mean \pm SEM). Data points represent individual organoids from 3 biological
661 replicates. $**P \leq 0.01$. (C) Expression levels of *Il6*/inflammatory response genes in organoid
662 culture (P0, day 14) from aging and young (undamaged) AP as determined by RT-qPCR (mean \pm
663 SEM). Data points represent biological replicates. (D) Bar graphs showing the (maximum)
664 number of AP organoid passage at present reached, grown in the absence (CTRL) or presence
665 of IL-6 (mean \pm SEM). Data points represent biological replicates. $*P \leq 0.05$; $**P \leq 0.01$; $****P \leq$
666 0.0001. (E) *Il6* gene expression levels in organoids from young and aging (damaged) AP at
667 consecutive passages (each at day 14 of culture) as determined by RT-qPCR. Bars show mean \pm
668 SEM and data points represent biological replicates. $*P \leq 0.05$; $**P \leq 0.01$.